Influence of seasonal and cyclic variations of thermospheric parameters on the nighttime intensity of the atomic oxygen red line

R.A. Kononov and A.V. Tashchilin

Institute for Solar-Terrestrial Physics,
Siberian Branch of the Russian Academy of Sciences, Irkutsk

Received September 17, 2001

According to observational data, the nighttime variation of the integral emission of the upper atmosphere in the red line (630 nm) at midlatitudes has a number of characteristic properties such as the emission growth during midnight and twilight periods. The appearance of these peculiarities depends on season and on the level of solar and geomagnetic activity. To study mechanisms of generation of the observed variations in the red emission the calculations of the variation of these values have been carried out based on the model of the ionosphere–plasmosphere interaction under different geophysical conditions (winter, spring, summer, fall, $F_{10,7}$ = 70, 130, 200). This model takes into account the nitric–oxygen cycle of chemical reactions, which is basic at altitudes higher than 100 km, and includes the ion composition (O^+, N^+, H^+, He^+, O_2^+, NO^+, N_2^+), temperatures of electrons and ions, photoelectron fluxes and horizontal neutral wind. Analysis of calculated results has made it possible to assess quantitatively the contribution of variations of the neutral composition, wind velocity, and conditions of the emission to the formation of the observed night emissions of atomic oxygen at the 630-nm line.

Introduction

The red-line emission at λ = 630 nm is one of the main types of emissions of the nighttime mid-latitude thermosphere. The emission occurs due to the forbidden transition ($^1D \rightarrow {}^3P_2$) of atomic oxygen and is formed at heights above 120 km, i.e., at the altitudes of F-region of the ionosphere. The oxygen red line emission intensity is an indicator of the ionosphere–thermosphere interaction, and its variations are uniquely connected both with the electron concentration and temperature in the region of F_2-layer of the ionosphere and with the concentration of neutral component of the upper atmosphere. At present, a great bulk of observational data of 630-nm emission in a wide range of heliogeophysical conditions has been accumulated. The conditions include the quiet and geomagnetic disturbed periods.[1,2]

At the geophysical observatory of the Institute for Solar-Terrestrial Physics SB RAS in the settlement of Tory during recent few years the intrinsic night emission of the Earth's atmosphere, in particular, of the atomic oxygen red line in mid-latitudes are being observed and recorded.

The goal of this paper is to present some results of the red line emission observation under geomagnetically quiet conditions as well as to interpret these data based on the model of the mid-latitude ionosphere developed.

Results of observations

Variations of the emission at λ = 630 nm are characterized by a regular night behavior. At nighttime the 630-nm emission intensity is centered in the ionospheric F region with the intensity maximum at the heights about 250–270 km. The 630 nm emission intensity during all seasons decreases from 200–300 rayleigh (R) to 30–50 R at about midnight. Until 22–23 local time, the emission intensity decreases reasonably fast, then slows down and after midnight varies slightly till the time when the local twilight begins (for spring, summer, fall), or till the point in time of pre-twilight amplification connected with the beginning of twilight in the magnetic-conjugate ionosphere (for winter).[1]

Typical time variations of the emission intensity of 630-nm line under quiet geophysical conditions, observed at nighttime, are shown in Fig. 1.

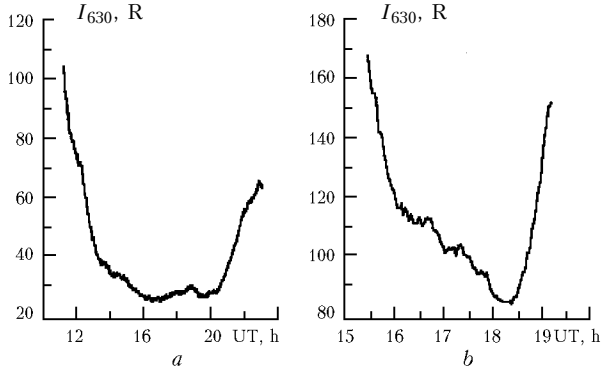

Fig. 1. Representative nighttime emission behavior at λ = 630 nm for winter, January 10, 2000 (*a*) and for summer, June 7, 2000 (*b*).

It is seen that for winter period (Fig. 1*a*) after 22 LT (14 UT) the following peculiarities of the

0235-6880/01/10 902-03 $02.00

behavior of 630 nm emission intensity are typical: the long, about 4–5 hours of nighttime stage of slight variations, after which at 3.5–4.5 hours the amplification of emission intensity begins, which changes to a small "step" (the greatest duration of which falls on the period of winter solstice) and further, when the local sunrise begins, the enhanced growth of emission intensity starts. For summer period (Fig. 1*b*) the intensity decrease characteristic of the night behavior is typical up to 3 LT (the minimum falls on the period of summer solstice) and also the increase in the radiation intensity as compared with the winter period. The nighttime behavior in spring and fall seasons is intermediate between the summer and winter behaviors. Besides, the night behavior of 630-nm emission at an observation point is often distorted by irregular variations caused by local disturbances in the night atmosphere and under unfavorable meteorological conditions.

Interpretation of the observations

The integrated nighttime airglow intensity (in rayleighs) of the 630-nm line is determined by the expression

$$I_{630} = 10^{-6} \cdot A_{630} \int_0^\infty [O(^1D)]\mathrm{d}h\,, \qquad (1)$$

where $A_{630} = 0.0071\ s^{-1}$ is the Einstein coefficient; $[O(^1D)]$ is the concentration of excited oxygen atoms in ^1D state at an altitude h, whose value is determined from the balance condition between the pumping rate and devastation rate of the metastable level ^1D.

According to the present-day concepts,[3,4] the basic processes yielding the excitation of oxygen atoms to ^1D level are the following:

– dissociation recombination of molecular ions O_2^+:

$$O_2^+ + N_e \rightarrow O(^3P) + O(^1D); \qquad (2)$$

– the collisions with thermal electrons:

$$e_t + O(^3P) \rightarrow e_t + O(^1D); \qquad (3)$$

– the impacts of superheat electrons (photoelectrons):

$$e_{ph} + O(^3P) \rightarrow e_{ph} + O(^1D). \qquad (4)$$

Deactivation of atoms $O(^1D)$ occurs because of spontaneous emission (the probability A_{630}) and by beam suppression at the collisions with thermal electrons and neutral N_2 and O_2 molecules. From the condition of heat balance of excitation and deactivation processes we obtain the concentration $[O(^1D)]$ in the form

$$[O(^1D)] = \left[\frac{\gamma_1\xi_1[O_2^+]N_e + \gamma_2[O(^3P)][e_t] + \gamma_3[O(^3P)][e_{ph}]}{A_{630} + \gamma_4[O_2] + \gamma_5[N_2] + \gamma_6[O] + \gamma_7 N_e}\right], \qquad (5)$$

where ξ_1 is the coefficient of reaction (2) branching; γ_1, γ_2, and γ_3 are rate constants for reactions (2)–(4), respectively; γ_4, γ_5, γ_6, and γ_7 are rate constants for quenching reactions in collisions with O_2, N_2, O, and electrons, respectively.

Equation (5) for $[O(^1D)]$ incorporates the concentration N_e and the temperature T_e of thermal ionospheric plasma as well as the concentration of photoelectrons $[e_{ph}]$. To determine the altitude profiles of these values we used a theoretical model of the ionosphere–plasmosphere system developed at the Institute for Solar-Terrestrial Physics, SB RAS.

The model is based on the numerical solution of nonstationary equations of balance of particles and energy of thermal plasma in closed geomagnetic field tubes with the bases at 100 km altitude. It is assumed, that the plasma consists of atomic ions O^+, H^+, N^+, He^+ as well as molecular ions N_2^+, O_2^+, NO^+. Concentrations of all ions, besides N_2^+, are calculated taking into account the processes of photoionization, recombination, and diffusion along the geomagnetic field lines. Temperatures of electrons and ions are calculated taking into account processes of heat conductivity and energy exchange among electrons, ions, and neutrals, because of elastic and inelastic collisions. The rate of heating of thermal electrons by photoelectrons is calculated as solutions of kinetic transfer equation of photoelectrons in conjugate ionospheres taking the account of energy losses in passing through the plasmosphere.[5]

To describe the spatiotemporal variations of the temperature of the upper atmosphere and the concentrations of neutral components O, O_2, N_2, H, and N, we used a global empirical model of the thermosphere MSIS–86,[6] and the speed of horizontal thermospheric wind was determined by the HWM–90 model.[7] The ultraviolet radiation spectrum EUVAK[8] was used in calculating the photoionization rates of thermospheric components and power spectra of the initial photoelectrons. Detailed data on the model and method of numerical calculation can be found in Ref. 5.

To study the mechanisms of the formation of night variations of red line intensity, we have made the model calculations of integral emission (1) for a point with the geographic coordinates 52°N and 105°E for four seasons (spring, summer, fall, winter) and three levels of the solar activity ($F_{10.7}$ = 70, 130, 200).

The calculated results are shown in Fig. 2. Diagrams *a*, *c*, and *e* show the night behaviors of I_{630} for three seasons (data for the fall are identical with the spring data and therefore these data are not shown) at high (solid curves), mean (dot-and-dash curves), and low (dashed curves) levels of the solar activity. In the bottom panel of Fig. 2 (graphs *b*, *d*, *f*) the night behavior is presented of the integral intensity at a moderate activity ($F_{10.7}$ = 130) and the above three seasons corresponding to the mechanisms of D^1 level excitation at O_2^+ dissociation recombination (solid curves) as well as at collisions with the photoelectrons (dot-and-dash curves), and thermal electrons (dashed curves).

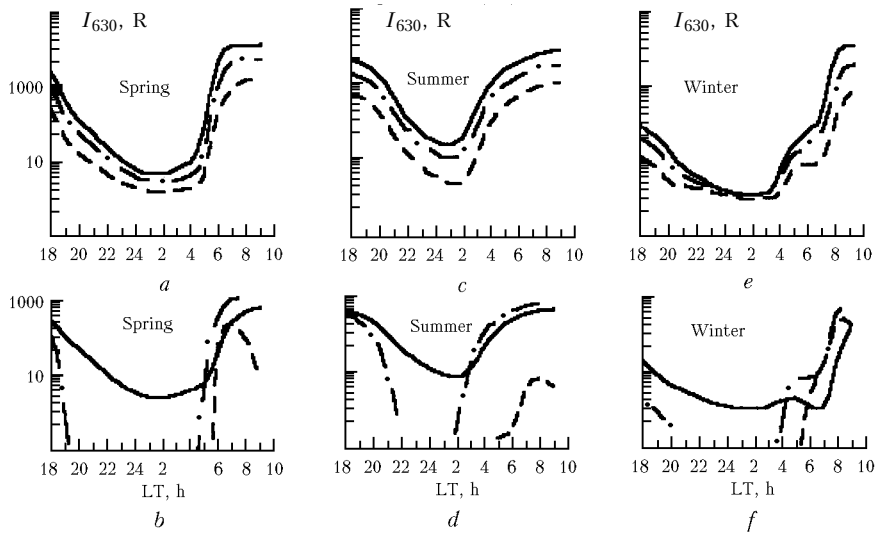

Fig. 2. Nighttime behavior of the emission at λ = 630 nm for the above-mentioned seasons and three levels of the solar activity: *a*, *c*, *e* – $F_{10.7} = 200$ (solid curves), $F_{10.7} = 130$ (dot-and-dash curves), $F_{10.7} = 70$ (dashed curves); *b*, *d*, *f* is the dissociative recombination (solid curves); photoelectrons (dot-and-dash curves), thermal electrons (dashed curves).

From the diagrams *a*, *c*, and *e* it follows that the night behavior of I_{630} shows considerable seasonal distinctions whereas with the increase of solar activity the uniform growth of the emittance occurs at all moments in time. At nighttime, the main mechanism of excitation is the dissociation recombination; in this case the corresponding emission intensity varies proportionally to N_e and $[O_2^+]$ variations (O_2^+ concentration falls down exponentially after the sunset). In spring and summer during twilight periods at sunrise and sunset, the contribution of photoelectron excitation becomes essential. This effect depends on the season because its action is limited by the moments of sunrise and sunset. It is precisely the increase of dark period when passing from summer to equinoctial seasons that causes a wider "gap" in the night behavior of I_{630} in spring as compared with that in summer (Figs. 2*a* and *c*). The thermal electron excitation is of minor importance in spring and summer.

In winter the nighttime behavior of I_{630} intensity has a qualitative peculiarity over a period before sunrise, which is expressed in the emission amplification about 3 hours before the local sunrise. As follows from Fig. 2*f*, this effect is also connected with the photoelectron excitation mechanism. It is a direct result of the relation between the conjugate ionospheres and is due to the arrival to the dark winter ionosphere superheat electrons from the conjugate summer ionosphere.

Thus the investigation of mechanisms of formation of the nighttime emission at λ = 630 nm has shown that:

1. Seasonal variations manifest themselves in the nighttime behavior of the integral emittance at λ = 630 nm more significantly than in the solar activity cycle;

2. Basic mechanisms of the emission generation at the red line of atomic oxygen are the dissociation recombination of O_2^+ and the collisional excitation of ^1D level by photoelectrons;

3. Constant characteristic of the nighttime behavior of I_{630} in winter is the extra enhancement of the emission by photoelectrons arriving from the conjugate summer ionosphere.

References

1. L.M. Fishkova, *Nocturnal Radiation of the Mid-Latitude Upper Earth's Atmosphere* (Metsniereba Press, Tbilisi, 1983), 272 pp.
2. P.B. Hays, D.W. Rusch, R.G. Roble, and I.G.G. Walker, Rev. Geophys. **16**, No. 2, 225–232 (1978).
3. S.C. Solomon, P.B. Hays, and V.I. Abreu, J. Geophys. Res. A **93**, No. 9, 9867–9882 (1988).
4. M.D. Burrage, C.G. Fesen, and V.I. Abreu, J. Geophys. Res. A **95**, No. 7, 10357–10364, (1990).
5. I.A. Krinberg and A.V. Tashchilin, *Ionosphere and Plasmosphere* (Nauka, Moscow, 1984), 192 pp.
6. A.E. Hedin, J. Geophys. Res. A **92**, No. 5, 4649–4662 (1987).
7. A.E. Hedin, M.A. Biondi, R.G. Burnside, R.M. Johnson, et al., J. Geophys. Res. A **96**, No. A5, 7657–7688 (1991).
8. P.G. Richards, I.A. Fennelly, and D.G. Torr, J. Geophys. Res. A **99**, No. A5, 8981–8992 (1994).